Intrinsic bounds of a two-qudit random evolution

A. Z. Khoury,[1] A. M. Souza,[2] L. E. Oxman,[1] I. Roditi,[2] R. S. Sarthour,[2] and I. S. Oliveira[2]
[1]*Instituto de Física, Universidade Federal Fluminense, 24210-346 Niterói, Rio de Janeiro, Brazil*
[2]*Centro Brasileiro de Pesquisas Físicas, Rua Doutor Xavier Sigaud 150, 22290-180 Rio de Janeiro, Rio de Janeiro, Brazil*

(Received 11 October 2017; published 26 April 2018)

We investigate entangled qudits evolving under random local SU(d) operations and demonstrate that this evolution is constrained by intrinsic bounds, showing robust features of two-qudit entangled states that can be useful for fault tolerant implementations of phase gates. Our analytical results are supported by numerical simulations and confirmed by experiments on nuclear magnetic resonance.

DOI: 10.1103/PhysRevA.97.042343

I. INTRODUCTION

The development of quantum technologies is challenged by the unavoidable action of the environment and uncontrollable experimental imperfections. These effects cause errors in quantum algorithms and limit the scalability of quantum devices. Strategies are in course to isolate the physical systems used for quantum information tasks and to identify features that are immune to those undesired effects. The use of engineered reservoirs [1–3], decoherence free subspaces [4], geometrical phases [5–16], topologically protected systems [17], and dynamical decoupling [18–21] has been considered as potential means for robust quantum computation. The role of entanglement in the geometric phase acquired by entangled quantum systems has motivated a great deal of interesting research works [22–24]. In particular, it has been theoretically predicted [25,26] and experimentally demonstrated [27,28] that the geometric phase acquired by maximally entangled qubits is discrete, restricted to integer multiples of π . Later, fractional phases were predicted for maximally entangled systems with arbitrary dimension d (qudits) [29–32] and for multiple qubits [33,34]. Quantum algorithms employing qudits have also been considered in the literature [35–37].

In this paper we demonstrate an intriguing feature regarding the evolution of entangled two-qudit states under arbitrary local SU(d) transformations, namely, the overlap between the transformed and the initial states is confined within a nontrivial boundary in the complex plane. This boundary is deduced analytically, confirmed by numerical simulations, and, furthermore, experimentally verified with nuclear magnetic resonance.

II. MATRIX STRUCTURE OF TWO-QUDIT STATES

Let us consider a two-qudit quantum state evolution

$$|\psi(t)\rangle = \sum_{i,j=1}^{d} M_{ij}(t)|ij\rangle, \tag{1}$$

where M is the coefficient matrix of the quantum state expansion in the computational basis $\{|ij\rangle\}$. It will be useful for our purposes, to write the coefficient matrix in its polar decomposition [38]:

$$M(t) = e^{i\theta(t)}\, Q(t)\, S(t), \tag{2}$$

where three sectors can be identified: (1) the U(1) sector represented by the overall phase factor $e^{i\theta(t)}$, (2) the SU(d) sector given by $S(t) \in \mathrm{SU}(d)$, and (3) the Hermitian sector $Q(t) = Q^{\dagger}(t)$. Under local unitary transformations, each sector follows an independent time evolution. Indeed, let $U_A(t) = e^{i\theta_A(t)}\bar{U}_A(t)$ and $U_B(t) = e^{i\theta_B(t)}\bar{U}_B(t)$ be the local unitary transformations applied to qudits A and B , with $\bar{U}_A(t)$ and $\bar{U}_B(t) \in \mathrm{SU}(d)$. In this case the evolution in each sector is given by

$$\begin{aligned} \theta(t) &= \theta(0) + \theta_A(t) + \theta_B(t), \\ Q(t) &= \bar{U}_A(t)\, Q(0)\, \bar{U}_A^{\dagger}, \\ S(t) &= \bar{U}_A(t)\, S(0)\, \bar{U}_B^{T}. \end{aligned} \tag{3}$$

It will be convenient to adopt the basis leading to the Schmidt decomposition of the initial state, so that $M_{ij}(0) = q_j\, \delta_{ij}$, where $\{q_j\} \in \mathbb{R}$ are the eigenvalues of the Hermitian sector in decreasing order $q_1 \geqslant q_2 \geqslant \cdots \geqslant q_d$. Of course, these eigenvalues are stationary since this sector undergoes a unitary transformation. The Schmidt decomposition also implies $\theta(0) = 0$ and $S(0) = \mathbb{1}$. Moreover, we shall assume that the two qudits are locally operated with SU(d) transformations ($\theta_A = \theta_B = 0$), making the U(1) sector stationary. Note that local SU(d) transformations are naturally realized in spin systems interacting with an external magnetic field, since the energies of the spin eigenstates are symmetrically shifted in this case. This makes nuclear magnetic resonance (NMR) the ideal platform for the experimental investigation.

For maximally entangled states, the Schmidt coefficients are all equal $q_j = 1/\sqrt{d}$ so that $Q(t) = \mathbb{1}/\sqrt{d}$ and the Hermitian sector remains stationary. In this case, the coefficient matrix structure will evolve solely in the SU(d) sector. For partial entanglement, the eigenvalues $\{q_j\}$ are unequal and the overlap evolution must be considered on both Hermitian and SU(d) sectors. We now demonstrate that this overlap remains restricted to a confined area of the complex plane the contour of which is given by the polar plot $R(\Phi)$ with $R \equiv |\langle\psi(0)|\psi(t)\rangle|$ and $\Phi \equiv \arg\langle\psi(0)|\psi(t)\rangle$. This contour depends on the dimension of the qudits and on the Schmidt

coefficients. In terms of the matrix structure, the overlap reads

$$\langle\psi(0)|\psi(t)\rangle = \mathrm{Tr}[Q(0)Q(t)S(t)]. \tag{4}$$

III. OVERLAP BOUNDARY

In order to derive the analytical shape of the contour, we must obtain the maximum value of R for fixed Φ to determine the contour function $R_{\max}(\Phi)$. The properties of the trace involving unitary and Hermitian matrices have been studied in a number of works [39–42]. However, little attention has been given to the case when the unitary matrices are restricted to SU(d). Properties of SU(3) traces were investigated in the context of the configuration space of lattice quantum chromodynamics [43]. More recently, the properties of SU(d) traces were studied in connection with quantum entropies as invariants for the projective unitary group acting on a finite-dimensional complex Hilbert space [44]. From these works, we learn that this kind of trace is maximized by diagonal unitary matrices that commute with $Q(0)$, leaving the Hermitian sector stationary. In this case, $Q(t) = Q(0)$ and the trace expression reduces to

$$\langle\psi(0)|\psi(t)\rangle = \sum_{j=1}^{d} q_j^2\, e^{i\phi_j(t)} = R\, e^{i\Phi}, \tag{5}$$

where the phase factors $e^{i\phi_j(t)}$ are the eigenvalues of $S(t)$. Since $\det S(t) = 1$, these phase factors are constrained by the condition

$$F(\{\phi_j\}) = \sum_{j=1}^{d} \phi_j = 0. \tag{6}$$

For a given configuration $\{\phi_j\}$, the overlap absolute value can be deduced from the real part of Eq. (5) as

$$R(\{\phi_j\}) = \sum_{j=1}^{d} q_j^2 \cos(\phi_j - \Phi). \tag{7}$$

Additionally, a second constraint can be immediately derived from the imaginary part:

$$G(\{\phi_j\}) = \sum_{j=1}^{d} q_j^2 \sin(\phi_j - \Phi) = 0. \tag{8}$$

We are now able to find $R_{\max}(\Phi)$ under constraints (6) and (8) using Lagrange multipliers. For this end, we define

$$L(\{\phi_j\},\lambda_f,\lambda_g) = R(\{\phi_j\}) + \lambda_f\, F(\{\phi_j\}) + \lambda_g\, G(\{\phi_j\}), \tag{9}$$

where λ_f and λ_g are Lagrange multipliers. The constrained extrema of R are obtained from the solutions of

$$\frac{\partial L}{\partial \phi_k} = q_k^2[-\sin(\phi_k - \Phi) + \lambda_g \cos(\phi_k - \Phi)] + \lambda_f = 0, \tag{10}$$

from which we readily derive the condition

$$q_k^2 \sin(\Phi + \theta - \phi_k) = \Lambda, \tag{11}$$

where the Lagrange multipliers were replaced by the more convenient variables $\theta = \arctan\lambda_g$ and $\Lambda = -\lambda_f \cos\theta$. Equations (6) and (8), plus condition (11) for $1 \leqslant k \leqslant d$, form a set of $d+2$ algebraic equations for the d individual phases ϕ_k plus the auxiliary variables Λ and θ.

A. General case

For partial entanglement, Eq. (11) can be solved in parametrized form as functions of $\gamma \equiv \Phi + \theta - \phi_d$. From condition (11) for $k = d$, we immediately get $\Lambda(\gamma) = q_d^2 \sin\gamma$. By inverting condition (11), adding it up for all k's, and using (6), we easily arrive at

$$\begin{aligned} \phi_k(\gamma) &= \frac{\Gamma}{d} - \arcsin\left(\frac{\Lambda}{q_k^2}\right) \qquad (1 \leqslant k \leqslant d-1), \\ \phi_d(\gamma) &= \frac{\Gamma}{d} - \gamma, \end{aligned} \tag{12}$$

where $\Gamma(\gamma) \equiv \gamma + \sum_{j=1}^{d-1} \arcsin(\Lambda/q_j^2)$ and the arcsin function is to be taken in the interval $[0,\pi/2]$ for $1 \leqslant k \leqslant d-1$. We can build the correspondence $R_{\max}(\gamma) \times \Phi(\gamma)$ by computing the parametric expressions

$$\begin{aligned} R_{\max}(\gamma) &= \left|\sum_{j=1}^{d} q_j^2 e^{i\phi_j(\gamma)}\right|, \\ \Phi(\gamma) &= \arg\left[\sum_{j=1}^{d} q_j^2 e^{i\phi_j(\gamma)}\right]. \end{aligned} \tag{13}$$

The Lagrange variables θ and Λ, and the auxiliary angle γ, have a clear geometric interpretation in the complex plane, as shown in Figs. 1(a) and 1(b) for qutrits, for example. Consider d phasors $q_k^2\, e^{i\phi_k}$ $(1 \leqslant k \leqslant d)$ rotating in the complex plane. Condition (11) imposes that the phasor arrow heads remain lined up during the evolution, as indicated by the red (online) line in Fig. 1(b). Due to condition (6), they cannot evolve all in the same sense, so one of the phasors must turn opposite to the others. The overlap acquires maximum absolute value for each phase Φ when the smallest phasor $q_d^2\, e^{i\phi_d}$ is the counter-rotating one and the remaining $d-1$ phasors rotate in the same sense, with all arrow heads lined up at all times. The Lagrange variable θ corresponds to the angle between the line connecting the arrow heads and the sum phasor $R_{\max}$, while Λ is the minimum distance from the origin of the complex plane to the connecting line.

By varying γ in the interval $[0,2d\pi]$, we can draw the polar plot of the overlap boundary in the complex plane. This boundary defines a closed curve with exactly d branches covered by the intervals $\gamma \in [2n\pi,2(n+1)\pi]$ $(0 \leqslant n \leqslant d-1)$. When $\gamma = 2n\pi$, a closed evolution $(|\psi(0)\rangle \to e^{i\Phi}|\psi(0)\rangle)$ is completed, so that the maximum overlap modulus reaches unity and its phase assumes the discrete values $\Phi = 2n\pi/d$ that correspond to the topological phases allowed for two-qudit closed evolutions. The minimum value of $R_{\max}$ is $1 - 2q_d^2$ when $\gamma = (2n+1)\pi$ so that $\Phi = (2n+1)\pi/d$. The sharp edges between the boundary branches exhibited by maximally entangled states are smoothened as q_d diminishes until the boundary degenerates to the unit circle when $q_d = 0$, as

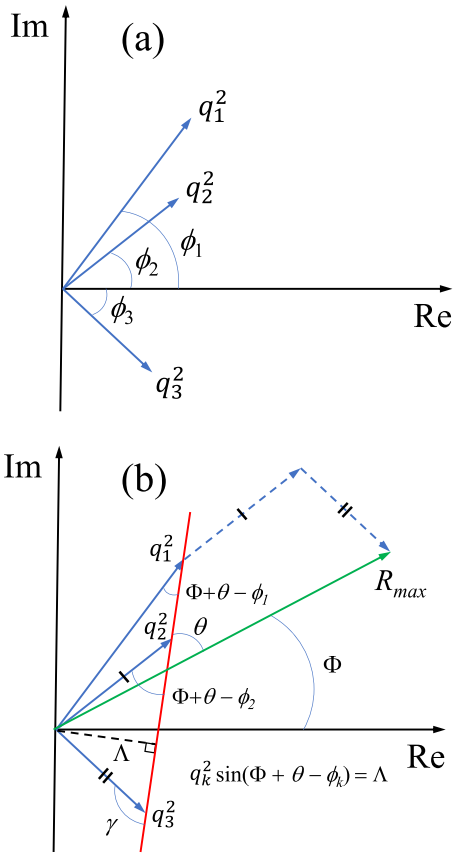

FIG. 1. (a) Graphic representation in the complex plane of the summation terms in Eq. (13) for qutrits. (b) Geometric interpretation of the Lagrange variables and condition (11). The smallest phasor (q_3^2) rotates opposite to the remaining ones, with all arrow heads lined up (red line) at all times. The Lagrange variable θ corresponds to the angle between the line connecting the arrow heads and the sum phasor $R_{\max}$, while Λ is the minimum distance from the origin to the connecting line. Condition (11) identifies Λ as the projection of all phasors on the direction perpendicular to the connecting line.

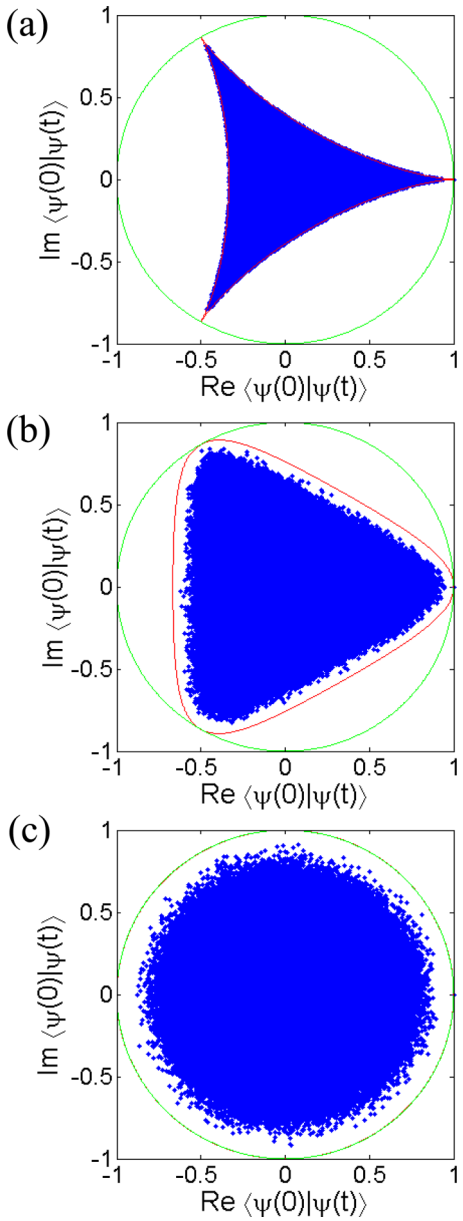

FIG. 2. Evolution of the two-qutrit overlap under random local SU(3) operations for (a) maximally entangled qutrits $q_1^2 = q_2^2 = q_3^2 = 1/3$, (b) partially entangled qutrits with $q_1^2 = 1/2$, $q_2^2 = 1/3$, $q_3^2 = 1/6$, and (c) partially entangled qutrits with $q_1^2 = 2/3$, $q_2^2 = 1/3$, $q_3^2 = 0$. The analytical boundary is displayed in red (online) and the results of numerical simulations are displayed in blue (online) dots. The unit circle is indicated in green (online) line for reference. In (c) the analytical boundary coincides with the unit circle.

clearly shown in Figs. 2(b) and 2(c). The numerical simulations with random SU(3) × SU(3) matrices also demonstrate clear confinement. However, the diagonal evolutions defining the boundary are statistically untypical, so that points approaching the boundary are rare. Of course, the confinement region is completely covered when the random unitaries are sampled among the diagonal ones, as we have numerically verified. This kind of statistical gap does not show up for maximally entangled states, because the overlap is reduced to the trace of the SU(d) matrix $S(t)$ [in this case $Q(t) \propto \mathbb{1}$], which is solely determined by its eigenvalues independently of being diagonal or not.

B. Maximally entangled qudits

A simple analytical expression can be obtained for maximally entangled qudits ($q_k = 1/\sqrt{d}$). In this case, all ϕ_k's for $1 \leqslant k \leqslant d-1$ are equal, $\phi_k = \phi$, and $\phi_d = -(d-1)\phi$. Then, the parametric expressions (13) for the maximum overlap modulus and phase reduce to

$$\begin{aligned} R_{\max}(\phi) &= \frac{1}{d}\left|(d-1)e^{i\phi} + e^{-i(d-1)\phi}\right| \\ &= \sqrt{1 - 4\left(\frac{d-1}{d^2}\right)\sin^2\left(\frac{d\,\phi}{2}\right)}, \\ \Phi(\phi) &= \arg[(d-1)e^{i\phi} + e^{-i(d-1)\phi}] \\ &= \phi + \arg\left(d - 1 + e^{-id\phi}\right). \end{aligned} \tag{14}$$

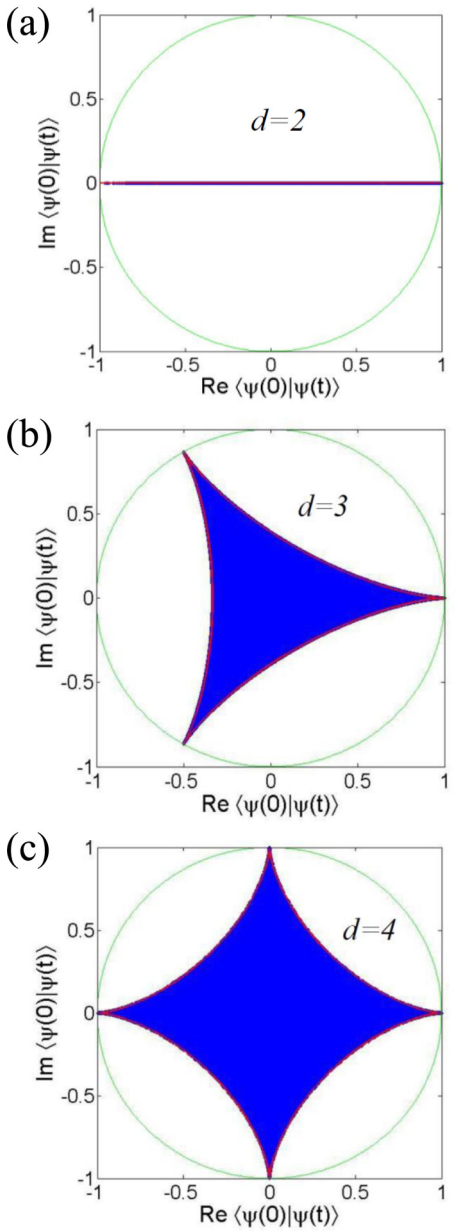

FIG. 3. Evolution of the two-qudit overlap under random local SU(d) operations for (a) $d = 2$, (b) $d = 3$, and (c) $d = 4$. The analytical boundary is displayed in red (online) and the results of numerical simulations are displayed in blue (online) dots. The unit circle is indicated in green (online) for reference.

In order to illustrate the overlap boundaries for different dimensions, we present in Figs. 3(a) and 3(b) the analytical contours given by Eqs. (14) (red line curves) and the numerical simulations with random SU(d) × SU(d) transformations (blue line dots) for $d = 2$ and 3. The minimum value of $R_{\max}$ is $1 - 2/d$, so that for qubits the overlap boundary collapses to a line segment defined by the interval $[-1,1]$ on the real axis, as clearly shown in Fig. 3(a). The limiting contour for $d = 3$ is displayed in Fig. 3(b). The numerical results show strict confinement within the analytical boundary in both cases. Moreover, note that $R_{\max}$ reaches unity when the overlap phase assumes the allowed topological phases for qudits: $\Phi = 2n\pi/d$.

C. Qubits

Simple analytical expressions for $R_{\max} \times \Phi$ can also be derived for qubits with arbitrary entanglement. This will be particularly convenient for our experimental investigation. For a pair of qubits initially prepared in a pure state with Schmidt decomposition $|\psi(0)\rangle = q\,|00\rangle + \sqrt{1-q^2}\,|11\rangle$, the concurrence is $C = 2q\sqrt{1-q^2}$, and Eqs. (13) reduce to

$$\begin{aligned} R_{\max} &= |q^2 e^{i\phi} + (1-q^2)e^{-i\phi}| \\ &= \sqrt{1 - C^2 \sin^2\phi}, \\ \Phi &= \arg[q^2 e^{i\phi} + (1-q^2)e^{-i\phi}] \\ &= \arctan(\sqrt{1-C^2}\,\tan\phi). \end{aligned} \tag{15}$$

For product states ($C = 0$), one trivially obtains $R_{\max} = 1$ and $\Phi = \phi$, which corresponds to the unit circle boundary. For maximally entangled states ($C = 1$), we have $R_{\max} = |\cos\phi|$ and Φ becomes discrete, assuming only zero or π. Note that the minimum value of $R_{\max}$ is equal to $\sqrt{1-C^2}$, so that the concurrence can be inferred from the contour of the boundary region.

IV. TWO-QUBIT TOPOLOGICAL PHASE STABILITY

There is a remarkable difference between qubits and qudits ($d > 2$) in what regards the phase stability of entangled states under random local SU(d) operations. Since the overlap boundary for maximally entangled qubits collapses to a segment on the real axis, the two-qubit state can only acquire discrete phase values of zero or π in either open or closed evolutions. Moreover, the π phase shift requires a drastic change in the initial quantum state, that cannot be caused by sources of small unitary noise. In this way, the phase of a two-qubit quantum state becomes more stable as entanglement is increased. We will demonstrate this interesting feature first with numerical simulations and then with a NMR experiment.

The situation is completely different for higher dimensions, since the quantum state overlap can be randomly driven inside a finite area of the complex plane. In an open evolution, even maximally entangled two-qudit states can acquire any random phase in the full interval $[0,2\pi]$, although closed evolutions are restricted to the discrete topological phases $2n\pi/d$ ($n \in \mathbb{Z}$).

In order to investigate the phase stability, we will simulate the quantum state evolution of qubits ($d = 2$) and qutrits ($d = 3$) under random sequences of infinitesimal unitary transformations of the form $dU_A \otimes dU_B$ given by

$$\begin{aligned} dU_A &= \mathbb{1} + i\,dt \sum_{n=1}^{d^2-1} a_n T_n, \\ dU_B &= \mathbb{1} + i\,dt \sum_{n=1}^{d^2-1} b_n T_n, \end{aligned} \tag{16}$$

where T_n are the $d^2 - 1$ generators of SU(d) (Pauli matrices for qubits and Gelmann matrices for qutrits), a_n and b_n are Gaussian-distributed random numbers, and dt is the dimensionless time step. The two-qudit quantum state is evolved

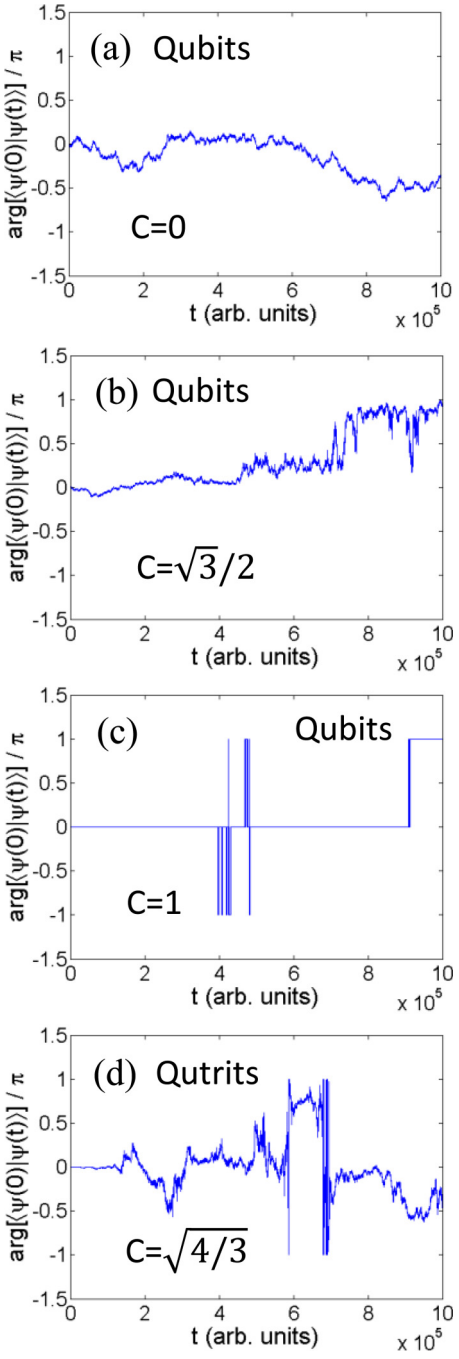

FIG. 4. Time evolution of the two-qudit overlap under random local SU(d) operations for (a) qubits with $C = 0$, (b) qubits with $C = \sqrt{3}/2$, (c) maximally entangled qubits ($C = 1$), and (d) maximally entangled qutrits ($C = \sqrt{4/3}$).

according to

$$|\psi(t+dt)\rangle = dU_A \otimes dU_B |\psi(t)\rangle \tag{17}$$

and the overlap phase $\arg[\langle\psi(0)|\psi(t)\rangle]$ is computed as a function of time.

In Fig. 4 we display typical time series of the overlap phase. The increased stability of maximally entangled qubits is clear from Figs. 4(a)–4(c). The phase fluctuations are reduced as the concurrence C is increased and becomes flat in a time scale when $C = 1$. In this case, the overlap phase remains stable until the random sequence of unitary kicks drives the two-qubit state towards the subspace orthogonal to $|\psi(0)\rangle$, when the overlap becomes small and fluctuates around zero. This fluctuation between small positive and negative real numbers causes a sequence of sudden jumps of the overlap phase between zero and π, as can be seen in Fig. 4(c). These sudden jumps cease when the quantum state moves away from the orthogonal subspace. In this sense, the two-qubit phase is piecewise stable for maximally entangled states. However, the same kind of phase stability cannot be seen in the time series shown in Fig. 4(d) for maximally entangled qutrits. In this case, the quantum state overlap can acquire any phase value inside $[0, 2\pi]$, as explained above.

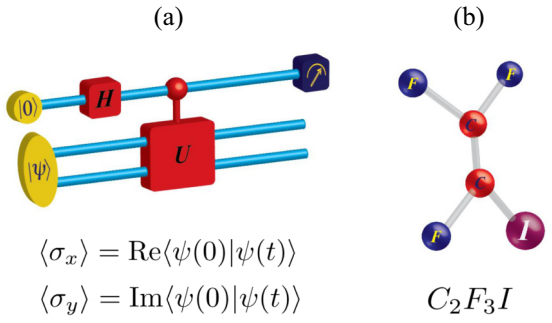

FIG. 5. (a) Quantum circuit for measurement of the two-qubit overlap. (b) The three-qubit iodotrifluoroethylene molecule.

V. NMR EXPERIMENT

In optical experiments, geometrical phases are only achievable using interferometric approaches. In NMR, the analog of interferometry can be implemented using the quantum circuit shown in Fig. 5(a), where the eigenstates of an auxiliary spin $-1/2$ emulate two photon paths [28,45–47]. In the beginning of the operation, the system we want to probe is prepared in a given two-qubit state $|\psi(0)\rangle$, whereas the auxiliary spin is prepared in the superposition state $(|0\rangle + |1\rangle)/\sqrt{2}$, by applying a Hadamard gate on the state $|0\rangle$. The application of the controlled unitary operator U provides the state $(|0\rangle|\psi(0)\rangle + |1\rangle|\psi(t)\rangle)/\sqrt{2}$, where $|\psi(t)\rangle = U|\psi(0)\rangle$. When a measurement is performed on the auxiliary spin, its normalized magnetization components on the x-y plane, which are proportional to the average value of the corresponding Pauli matrices, are directly related to the overlap between the states.

We used an ensemble of identical and noninteracting molecules in liquid state at room temperature, where nuclear spins are employed as qubits. The quantum state of the ensemble is prepared, from the thermal equilibrium, in the so-called pseudo-pure state (PPS) [51]:

$$\rho = (1-\epsilon)\frac{\mathbb{1}}{d} + \epsilon|\psi\rangle\langle\psi|. \tag{18}$$

Since the maximally mixed part $\mathbb{1}/d$ does not produce an observable signal, the overall NMR signal arises only from the pure state part $|\psi\rangle\langle\psi|$ where the factor $\epsilon \approx 10^{-5}$ is the thermal polarization and d is the dimension of the Hilbert space. Under a suitable normalization, the state (18) is equivalent to that from

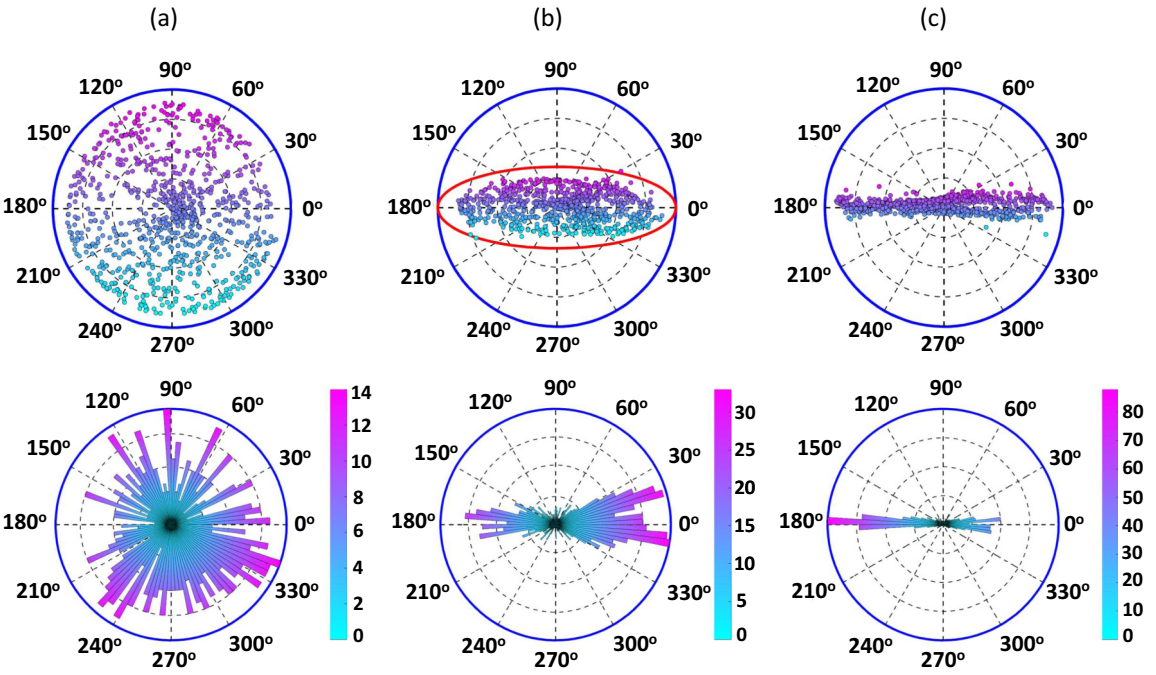

FIG. 6. Experimental overlap under random unitary evolutions for three different states: (a) the separable state $|00\rangle$ ($C = 0$), (b) the partially entangled state $\cos(7\pi/36)\,|00\rangle + \sin(7\pi/36)\,|11\rangle$ ($C = 0.94$), and (c) the maximally entangled state $(|00\rangle + |11\rangle)/\sqrt{2}$ ($C = 1$). The top panel shows the overlap $\langle\psi(0)|\psi(t)\rangle$ in the complex plane and the bottom panel shows the phase distributions in polar histograms. The phase concentration around the discrete values zero and π is clear for maximally entangled states.

a system in a pure state $|\psi\rangle$ and, therefore, can be used to test different features of pure entangled states [52–54].

The experiment was performed at room temperature, using a 500-MHz Varian NMR spectrometer and an ensemble of iodotrifluoroethylene (C_2F_3I) molecules dissolved in deuterated acetone. This molecule [see Fig. 5(b)] contains three spin-1/2 ^{19}F nuclei where two fluorine nuclei are used to encode the state $|\psi\rangle$ and one fluorine nucleus is used as the auxiliary spin. The PPS was created using the control transfer gates technique [55]; the actual pulse sequence used can be found in [47]. To implement gate operations we exploit standard Isech shaped pulses interleaved with periods of free evolutions. For combining all operations into a single pulse sequence we have used the techniques described in [48–50].

Figure 6 shows the overlap $\langle\psi(0)|\psi(t)\rangle$ in the complex plane under 800 random unitaries for three states with different degrees of entanglement. The unitaries were applied only on a single qubit of the entangled pair and have the form of combined rotations $U = R_x(\theta)R_z(\beta)$ around the x and z axes, where θ and β were randomly chosen from zero to 4π. The results clearly show the confinement by the bounds predicted by Eq. (15), indicated in red (online) in Fig. 6(b). As the degree of entanglement is increased, the confinement effect becomes more pronounced and the acquired geometrical phase becomes more robust, being almost strictly restricted to only zero or π when the state is maximally entangled. The phase distribution histograms are shown in the bottom panel of Fig. 6. They confirm the statistical concentration of the phase distribution around the discrete phases when entanglement is increased. The small deviations from the theory are due to decoherence processes and experimental imperfections on the control gates.

VI. CONCLUSION

In conclusion, we have investigated pairs of entangled qudits evolving under random local SU(d) operations. We have analytically demonstrated that the overlap between the SU(d) transformed and the initial state is confined within boundaries that only depend on the degree of entanglement. This feature was confirmed by numerical simulations with random local unitaries and, moreover, experimentally verified with an NMR setup. Our results provide a step further in the direction of robust quantum computation by demonstrating a noise resistant phase acquired by entangled qubits.

ACKNOWLEDGMENTS

Funding was provided by Coordenação de Aperfeiçoamento de Pessoal de Nível Superior, Fundação de Amparo à Pesquisa do Estado do Rio de Janeiro, Instituto Nacional de Ciência e Tecnologia de Informação Quântica, and Conselho Nacional de Desenvolvimento Científico e Tecnológico.

[1] N. A. Peters, J. B. Altepeter, D. A. Branning, E. R. Jeffrey, T.-C. Wei, and P. G. Kwiat, Phys. Rev. Lett. **92**, 133601 (2004).

[2] A. Aiello, G. Puentes, and J. P. Woerdman, Phys. Rev. A **76**, 032323 (2007).

[3] M. Hor-Meyll, A. Auyuanet, C. V. S. Borges, A. Aragão, J. A. O. Huguenin, A. Z. Khoury, and L. Davidovich, Phys. Rev. A **80**, 042327 (2009).

[4] G. M. Palma, K. A. Suominen, A. K. Ekert, Proc. R. Soc. A **452**, 567 (1996).

[5] J. A. Jones, V. Vedral, A. Ekert, and G. Castagnoli, Nature (London) **403**, 869 (2000).

[6] D. Leibfried, B. De Marco, V. Meyer, D. Lucas, M. Barrett, J. Britton, W. M. Itano, B. Jelenković, C. Langer, T. Rosenband, and D. J. Wineland, Nature (London) **422**, 412 (2003).

[7] A. Greilich, S. E. Economou, S. Spatzek, D. R. Yakovlev, D. Reuter, A. D. Wieck, T. L. Reinecke, and M. Bayer, Nat. Phys. **5**, 262 (2009).

[8] G. Feng, G. Xu, and G. Long, Phys. Rev. Lett. **110**, 190501 (2013).

[9] A. A. Abdumalikov, J. M. Fink, K. Juliusson, M. Pechal, S. Berger, A. Wallraff, and S. Filipp, Nature (London) **496**, 482 (2013).

[10] K. Toyoda, K. Uchida, A. Noguchi, S. Haze, and S. Urabe, Phys. Rev. A **87**, 052307 (2013).

[11] S. Arroyo-Camejo, A. Lazariev, S. W. Hell, and G. Balasubramanian, Nat. Commun. **5**, 4870 (2014).

[12] C. Zu, W.-B. Wang, L. He, W.-G. Zhang, C.-Y. Dai, F. Wang, and L.-M. Duan, Nature (London) **514**, 72 (2014).

[13] L. Wang, T. Tu, B. Gong, C. Zhou, and G.-C. Guo, Scientific Reports **6**, 19048 (2016).

[14] C. G. Yale, F. J. Heremans, B. B. Zhou, A. Auer, G. Burkard, and D. D. Awschalom, Nat. Photon. **10**, 184 (2016).

[15] Y. Sekiguchi, N. Niikura, R. Kuroiwa, H. Kano, and H. Kosaka, Nat. Photon. **11**, 309 (2017).

[16] Z. Zhang, T. Wang, L. Xiang, J. Yao, J. Wu, and Y. Yin, Phys. Rev. A **95**, 042345 (2017).

[17] A. Kitaev, Ann. Phys. (NY) **303**, 2 (2003).

[18] J. Zhang, A. M. Souza, F. D. Brandao, and D. Suter, Phys. Rev. Lett. **112**, 050502 (2014).

[19] A. M. Souza, G. A. Alvarez, and D. Suter, Phys. Rev. Lett. **106**, 240501 (2011).

[20] A. M. Souza, G. A. Alvarez, and D. Suter, Phys. Rev. A **86**, 050301(R) (2012).

[21] A. M. Souza, R. S. Sarthour, I. S. Oliveira, and D. Suter, Phys. Rev. A **92**, 062332 (2015).

[22] E. Sjöqvist, Phys. Rev. A **62**, 022109 (2000).

[23] B. Hessmo and E. Sjöqvist, Phys. Rev. A **62**, 062301 (2000).

[24] E. Sjöqvist, Int. J. Quantum Chem. **115**, 1311 (2015).

[25] P. Milman and R. Mosseri, Phys. Rev. Lett. **90**, 230403 (2003).

[26] P. Milman, Phys. Rev. A **73**, 062118 (2006).

[27] C. E. R. Souza, J. A. O. Huguenin, P. Milman, and A. Z. Khoury, Phys. Rev. Lett. **99**, 160401 (2007).

[28] J. Du, J. Zhu, M. Shi, X. Peng, and D. Suter, Phys. Rev. A **76**, 042121 (2007).

[29] L. E. Oxman and A. Z. Khoury, Phys. Rev. Lett. **106**, 240503 (2011).

[30] A. Z. Khoury, L. E. Oxman, B. Marques, A. Matoso, and S. Pádua, Phys. Rev. A **87**, 042113 (2013).

[31] A. Z. Khoury and L. E. Oxman, Phys. Rev. A **89**, 032106 (2014).

[32] A. A. Matoso, X. Sánchez-Lozano, W. M. Pimenta, P. Machado, B. Marques, F. Sciarrino, L. E. Oxman, A. Z. Khoury, and S. Pádua, Phys. Rev. A **94**, 052305 (2016).

[33] M. Johansson, M. Ericsson, K. Singh, E. Sjöqvist, and M. S. Williamson, Phys. Rev. A **85**, 032112 (2012).

[34] M. Johansson, A. Z. Khoury, K. Singh, and E. Sjöqvist, Phys. Rev. A **87**, 042112 (2013).

[35] S. S. Bullock, D. P. O'Leary, and G. K. Brennen, Phys. Rev. Lett. **94**, 230502 (2005).

[36] A. Muthukrishnan, and C. R. Stroud, Jr., Phys. Rev. A **62**, 052309 (2000).

[37] R. Ionicioiu, T. P. Spiller, and W. J. Munro, Phys. Rev. A **80**, 012312 (2009).

[38] P. R. Halmos, in *A Hilbert Space Problem Book*, Graduate Texts in Mathematics Vol. 19 (Springer, New York, 1982).

[39] J. von Neumann, Tomsk. Univ. Rev. **1**, 286 (1937).

[40] H. A. L. Kiers and J. M. F. Ten Berge, Linear Algebra and its Applications **126**, 125 (1989).

[41] L. Chen and C. S. Wong, Linear Algebra and its Applications **171**, 109 (1992).

[42] N. Komaroff, Linear Algebra and its Applications **428**, 738 (2008).

[43] S. Charzyński, J. Kijowski, G. Rudolph, and M. Schmidt, J. Geom. Phys. **55**, 137 (2005).

[44] W. Slomczyński and A. Szczepanek, IEEE Trans. Inf. Theory **63**, 7821 (2017).

[45] D. Suter, K. T. Mueller, and A. Pines, Phys. Rev. Lett. **60**, 1218 (1988).

[46] A. Ghosh and A. Kumar, Phys. Lett. A **349**, 27 (2006).

[47] F. Anvari Vind, A. Foerster, I. S. Oliveira, R. S. Sarthour, D. O. Soares-Pinto, A. M. Souza, and I. Roditi, Scientific Reports **6**, 20789 (2016).

[48] M. D. Bowdrey, J. A. Jones, E. Knill, and R. Laflamme, Phys. Rev. A **72**, 032315 (2005).

[49] C. A. Ryan, C. Negrevergne, M. Laforest, E. Knill, and R. Laflamme, Phys. Rev. A **78**, 012328 (2008).

[50] A. M. Souza, J. Zhang, C. A. Ryan, and R. Laflamme, Nat. Commun. **2**, 169 (2011).

[51] I. S. Oliveira, T. J. Bonagamba, R. S. Sarthour, J. C. C. Freitas, and E. R. de Azevedo, *NMR Quantum Information Processing* (Elsevier, Amsterdam, 2007).

[52] A. M. Souza, A. Magalhães, J. Teles, E. R. de Azevedo, T. J. Bonagamba, I. S. Oliveira, and R. S. Sarthour, New J. Phys. **10**, 033020 (2008).

[53] C. Ren, D. Lu, M. Shi, X. Peng, and J. Du, Phys. Lett. A **373**, 4222 (2009).

[54] R. J. Nelson, D. G. Cory, and S. Lloyd, Phys. Rev. A **61**, 022106 (2000).

[55] M. Kawamura, B. Rowland, and J. A. Jones, Phys. Rev. A **82**, 032315 (2010).